Volume 9, Issue 5, 2019, 4340 - 4344 ISSN 2069-5837

Biointerface Research in Applied Chemistry

www.BiointerfaceResearch.com

https://doi.org/10.33263/BRIAC95.340344

Original Research Article Open Access Journal

Received: 21.08.2019 / Revised: 01.10.2019 / Accepted: 03.10.2019 / Published on-line: 08.10.2019

Antimicrobial effect, electronic and structural correlation of nano-filled Tin Bismuth metal alloys for biomedical applications

Raghda Abou Gabal [1,*], Rizk Moustafa Shalaby [2], Amr Abdelghany [3], Mustafa Kamal [2]

[1]Mansoura Urology and Nephrology Center, Mansoura University, Mansoura, 35516, Egypt

[2]Physics Department, Faculty of Science, Mansoura University, Mansoura, 35516, Egypt

[3]Spectroscopy Department, Physics Division, National Research Center, 33 Elbehouth St., Dokki, 12311, Cairo, Egypt

*corresponding author e-mail address: ***raghdaabogabal@gmail.com***

ABSTRACT

In this work silver vanadate ($AgVO_3$) nano-rods were successfully synthesized using chemical precipitation route and doped in hypo (Sn 99%- Bi 1%) and hyper (Sn 3%- Bi 97%) -eutectic tin-bismuth (Sn-Bi) alloy. Nanostructured metal alloy was synthesized using powder compact metallurgy technique as a new low cost and time-consuming route. Effects of the $AgVO_3$ nano-rods content on the band structure of (Sn-Bi) alloy has been investigated through electronic transition studied via ATR ultraviolet/visible spectrophotometric and Hall Effect measurements. Antimicrobial studies for pathogenic Gram negative as well as Gram positive bacteria were also investigated and correlated to the analyzed electronic and optical properties. The work a debate avenue for probability controllingthe microbial growth and to correlate electronic properties of (Sn-Bi) alloy along with their antimicrobial properties.

Keywords: *Silver vanadate; Sn-Bi Alloy; Powder metallurgy ; Hall Effect; Antibacterial.*

1. INTRODUCTION

During last decade a revolution of material science employ new material in the form of composite, blend, alloy an nanomaterials with superior properties for specific uses in different fields [1, 2,3].

In the field of medicine [4], metal alloy world witnessing a great progression of novel multidisciplinary technologies[5], especially in the memory shape, biosensing [6] and many other biological applications [7, 8]. Alloys containing nanomaterials represent a class of nanostructured alloys that play an important role in such field [9]. These alloys acquire antibacterial properties that may serve in manufacturing antibacterial surfaces in hospitals and other work places exposed to antibacterial contamination.

Bacteria response to nanoparticles (NPs) directly depends on the structure of the bacterial cell wall. The Bacteria categorized based on its structure and function to Gram positive (+) and Gram negative (-). The wall of Gram positive has a thick layer of peptidoglycan attached to teichoic acids that found only in Gram (+) [10] while the wall of the Gram negative has a thin layer of peptidoglycan. The outer membrane provides hydrophobic resistance and comprised of lipopolysaccrides that responsible for the negative charge of the cell membrane [11].

Harkes et al [12] postulated the differential resistance of the enteric Gram-negative bacilli due to ionic repulsion forces resulting from identical charges on the surface of the emulsion particles and bacteria. Silver vanadate nanoparticles ($Ag_2V_4O_{11}$) were tested for gas sensing performance applications and results showed relatively high sensitivity towards amines which are the main component of the cell wall [13]. *Ana Beatriz Vilela Teixeira* et al doped Endodontic Sealers with Nanoparticles of Silver Vanadate to acquire it antibacterial Effect and other Physicochemical Properties[14]. Not only the cell is the factor determine bacteria susceptibility to NPs, but also bacteria response differ from NPS to another, the growth rate, and the biofilm formation. It is hopeful that antibacterial properties may be attributed to the movement of holes and charges [15]. In this study (Sn-Bi), alloy act as a host for ($AgVO_3$) nanorods, for study nanorods effect on electronic properties of (Sn-Bi). Antibacterial properties [16,17] of metals may be attributed due to the reaction of holes and electrons with (OH^-, O_2) in water from radicals that in her turn may be lethal to bacteria or interact directly with the charges on the cell membrane, Since a metal sample with a nearly filled band is equivalent to a conductor in which the current is carried by positive holes, it is common that only one type of carrier is present, it is easy to find n direct from Hall coefficient. Its trail in the medical field to make composite metallic alloys reinforced with nano-particles and check its viability to use as an antimicrobial biomaterial.

In view of these criteria, the present study aims to introduce a targeted correlation between electronic structure of the studied alloy samples containing different mass fractions of nanoparticulate lamellar partner synthesized using cold pressing route by means of Hall measurements and the action towards pathogenic bacterial grams based on their cell wall structure.

2. MATERIALS AND METHODS

Tin powder supplied by WINLAB UK fine chemicals, Bismuth powder 100 mesh supplied by Aldrich Chemical Company, ammonium vanadate (NH_4VO_3) and ($AgNO_3$) supplied by Sigma Aldrich Co. Samples of nominal composition $x$$AgVO_3$-(100-$x$)[$Sn_{y\%}$-$Bi_{(100-y)\%}$] as y=(99, 3), x=(0,1,3,5,7) see Table 1 prepared from sample nomination and composition.

Chemical precipitation route was employed for the NPs preparation. An equal amount of (0.005M) aqueous solution of both ammonium vanadate *(*NH_4VO_3) and silver nitrate *(*$AgNO_3$*)* were added to each other and vigorously stirred at fixed pH (~ 4.6) until a yellow colored precipitate appeared. Final product washed several times before drying and final examination with transmission electron microscopy (TEM) and X-ray diffraction.

Table 1. sample nomination and composition.

	Hyper $xAgVO_3$-(100-x) [$Sn_{99\%}$-$Bi_{1\%}$]				Hypo $xAgVO_3$-(100-x) [$Sn_{3\%}$-$Bi_{97\%}$]		
	Sn	**Bi**	**$AgVO_3$**		**Sn**	**Bi**	**$AgVO_3$**
S0	99	1	0.00	**S10**	3.00	97.00	0.00
S1	98.57	0.43	1.00	**S11**	2.57	96.43	1.00
S2	98.71	0.29	3.00	**S12**	1.71	95.29	3.00
S3	98.85	0.15	5.00	**S13**	0.85	94.15	5.00
S4	98.99	0.01	7.00	**S14**	0.99	92.01	7.00

Pre-calculated mass fractions of supposed nanostructured metal alloy in the powdered form were mixed thoroughly for about 10 min in an agate mortar to ensure sample homogeneity before cold powder compaction. Equal amounts of all compositions were subjected to a high constant load of about (10 ton/cm^2) in an evocable die of diameter 1 cm. The samples were then expelled from the die and stored in a vacuum desiccator until use. Three samples of the same composition were used and averaged for each measurement.

Hall coefficient, mobility, conductivity end e/m ratio was recorded and calculated using Ecopia HMS - 5000 Hall Effect measurement system. Prepared metal alloy samples containing a different concentration of synthesized nanomaterial were measured in the form of compact discs of diameter 1 cm at ambient room temperature in an ordinary air atmosphere.

X-ray diffraction (XRD) data collected using PAN analytical X`Pert PRO occupied CuK_α radiation within the Bragg's angle (2θ) 4 to 80°. UV-Vis. optical recorded in the spectral range 190–2000 nm via JASCO-570 spectrometer IN ATR mode.

Minimum inhibition zone (MIZ) regime was engaged to examine the proposed antimicrobial activity of prepared nanostructured metal alloys. All samples were examined against a pathogenic gram bacteria (*Enteroococcus*, *Escherichia coli*, *Enterobacter* and *Klebsella*). The details of the method were previously published [18]. Data are estimated by SPSS 17.0 for windows(SpSs In., Chicago,IL, USA). Variables are expressed as mean ±Sd. The correlation of non-parametric parameters is obtained by spearmans correlation test. P values less than 0.05are considered to be
significant.

3. RESULTS

3.1. Characterization of synthesized silver vanadate nanorods

Figure 1 the obtained X-ray diffraction pattern of synthesized silver vanadate nanorods. The obtained pattern shows sharp characteristic intense peaks previously identified ((JCPDS 19-1151), (JCPDS 29-1154)) for α and β phases of crystalline silver vanadate. It was clear that α-phase represent a minor phase marked with * while major phase β marked with x. TEM image clarifies formation of nanorods (15-20 nm) diameter with a few micrometers length [19].

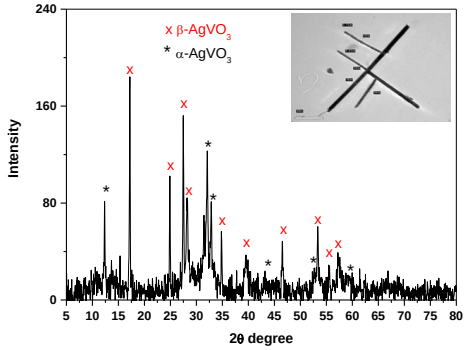

Figure 1. X-ray diffraction pattern and their TEM image.

3.2. Optical properties of the prepared nanostructured alloy.

The UV-visible reflectance spectra of the as-prepared samples are illustrated in Figure 2 a, b. The spectra of all the samples show good optical quality in the visible range due to the complete reflectance in the 500-800 nm range. Diffuse reflectance spectral studies in the UV-Vis-NIR region carried out to estimate the optical band gap of the composite metal alloy. The energy band gap of these materials estimated using the Kubelka-Munk remission function [20],

$$K = \left(\frac{(1-R)^2}{2R}\right)$$

according to Kubelka Munk K is reflectance transformed, R is reflectance (%), $\boldsymbol{hv}$ is the photon energy.

Optical energy gap can be calculated from extrapolated lines of the fundamental absorption edge shown in Figure 2. a, b and tabulated in Table 2.

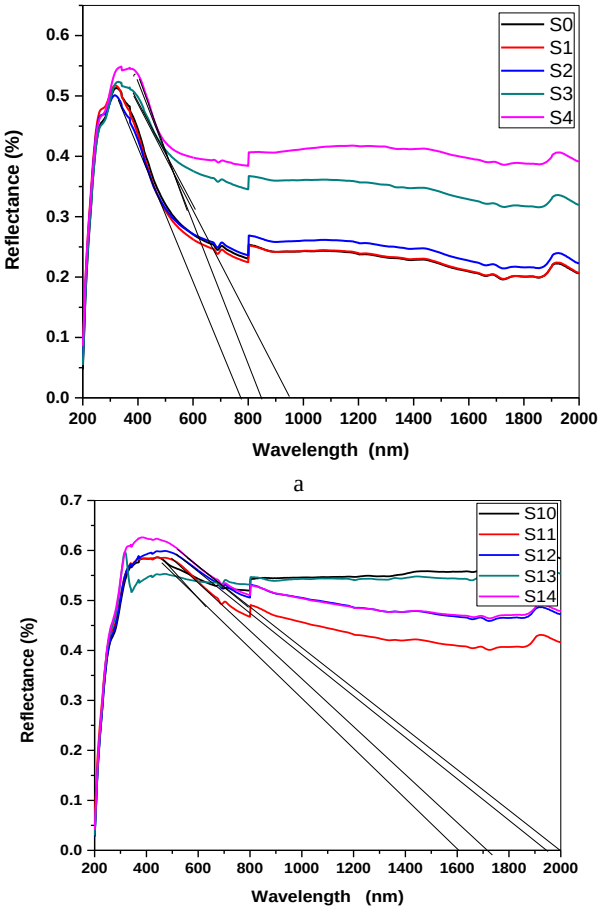

Figure 2. UV reflectance data of prepared samples.

Table 2. Calculated optical energy gap

Sample	E_g(eV)	Sample	E_g(eV)
S0	1.22	**S10**	0.77
S1	1.03	**S11**	0.73
S2	0.50	**S12**	0.64
S3	0.49	**S13**	0.63
S4	0.48	**S14**	0.62

It was clear that the value of the optical energy gap is strongly dependent on the content of silver vanadate added even in a minor concentration. The optical energy gap was found to be inversely proportional to the content of silver vanadate within the nanostructured alloy. This may be attributed to the size nature of add silver vanadate which increases the mobility of charge carriers and hence conduction or due to the tubular and lamellar shape of nanorods in both hyper and hypo-eutectic alloys.

3.3. Hall-effect measurements.

Hall Effect in metals and semiconductors considered puzzling, interesting and simple in principle because it exhibits a variety of different behaviors depending on whether the material was two, quasi-two or three dimensions, weak or strong scattering, magnetic or non-magnetic materials [21, 22]. Conductivity and Hall coefficients were measured in the intrinsic range of (Sn-Bi) alloy doped with ($AgVO_3$) nanorods. Observation of the Hall Effect permits experimental determination of the mean free path, mobility, electron concentration and decide the type of charge carrier (electrons or holes) responsible for conduction. In this experiment prepared sample in the solid state subjected to the electric and magnetic field perpendicular to each other to each other and to the face of the block.

Table 3 Hypereutectic alloy [$Sn_{99\%}$-$Bi_{1\%}$].

AgVO3 Content	Resistivity (Ω.m)	conductivity (1/(Ω.m)	Mobility (m2.V-1.S-1)	Hall coeff	e /m
control	1. E-07	6.85E+06	2.77E-03	-4.00E+00	1.54487E+18
1%AgVO	1.30E-07	7.70E+06	1.20E-01	1.50E-06	4.00011E+16
3%AgVO	1.05E-07	9.49E+06	4.55E-02	-4.70E-07	1.30416E+17
5%AgVO	6.75E-08	1.48E 07	3.81E-01	2.50E-06	2.43333E+16
7%AgVO	6.05E-08	1.65E+07	4.37E-01	2.60E-06	2.36614E+16

Table 4 Hypoeutictic alloys [$Sn_{3\%}$-$Bi_{97\%}$]

$AgVO_3$ Content	Resistivity (Ω.m)	conductivity (1/(Ω.m)	Mobility ($m_2.V^{-1}.S^{-1}$)	Hall coeff	e /m
control	7.55E-07	1.32E+06	1.29E-01	-9.71E+02	6.44E+15
1%AgVO	1.05E-06	9.56E+05	1.14E-01	-1.19E+02	5.26E+15
3%AgVO	1.16E-06	8.61E+05	6.67E-01	-7.75E+02	8.06E+14
5%AgVO	1.88E-06	5.31E+05	1.59E-02	-3.01E+02	2.09E+16
7%AgVO	3.00E-06	3.34E+05	1.65E-03	-4.94E+01	1.26E+17

Tables 3, 4 list the values of conductivity, Hall constant, Hall mobility, and electron concentration. It observed that some samples have a positive Hall coefficient; this can be explained based on the band theory of metals. It found that in this case, a traveling electron wave in the crystal will subject to a periodic variation in its potential energy, in the form of this variation will differ according to its direction in the crystal, therefore, the type of the atom and the symmetry of the crystal control the form and the periodicity of lattice potential.

The behavior of charge carrier in these samples studied under the combined influence of electric and magnetic fields as in Hall effect measurements Hall constant (R_H) its sign determine the sign of the charge of the current carrier either electrons or holes

3.4. Antibacterial result.

Agar plate method has been done to detect the antimicrobial activities of all studied samples. Four different test microbes represent gram negative and positive pathogenic bacteria; *Enteroococcus*, *Escherichia coli*, *Enterobacter* and *Klebsella* were selected to assess the antimicrobial activities. Performed tests grown on a nutrient agar medium (DSMZ1) diluted by sterilized double distilled water placed in sterilized Petri dishes containing an equal amount of solidified media. Studied samples placed on agar surface seeded with test microbes and incubated for 24 hrs adjusted at human body temperature (37 ± 2 °C). The diameter of the inhibition zone was recorded separately for each sample. Figure 3. a, b reveal the relationship between the concentration of added silver vanadate nanorods in hyper and hypo-eutectic alloys and measured diameter of inhibition zone for each pathogenic bacteria.

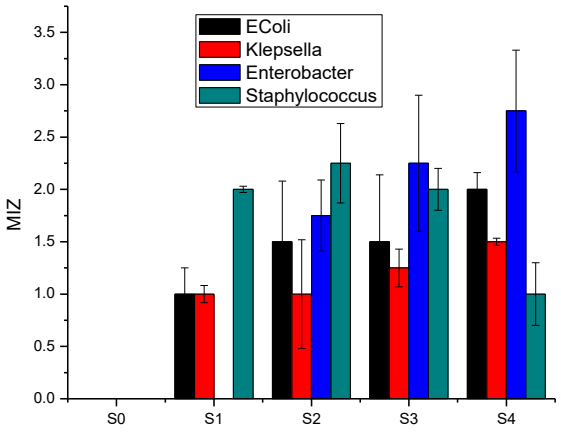

a

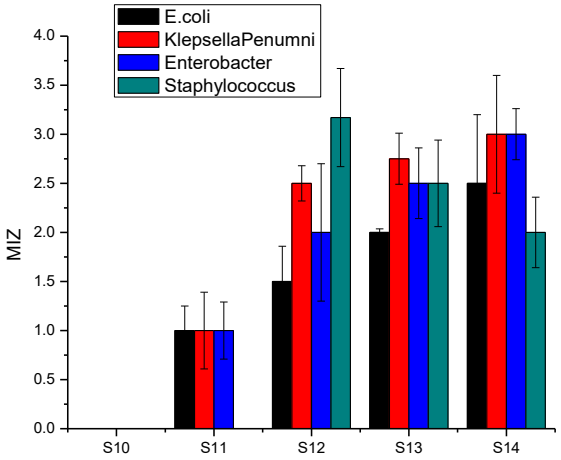

b

Figure 3 MIZ versus silver vanadate content for different pathogenic bacteria in hyper and hypo-eutectic Tin-Bismuth alloys.

In hypereutectic samples **[$Sn_{99\%}$-$Bi_{1\%}$]**, holes are responsible for charge transfer expect control and 3%$AgVO_3$ samples that have negative charges. *E.coli*, *klepsella pnemnia*,

Enterobacter have a significant positive correlation between diameter zone and hall effect with variation of P and r due to presence of biofilm or alteration the composition of the cell wall instead of, Staphylococcus (Gram+) has a negative correlation expect for S_2 as electrons are charge carrier in this sample represented in Fig 3.In hypoeutectic samples [$Sn_{3\%}$-$Bi_{97\%}$], R_H of samples is negative indicating that current is carried by electrons Gram (-) bacteria have a negative correlation between diameter zone and Hall effect with a variation of P, r, in contrast to Staphylococcus Gram(+) that has a positive correlation for all samples.

4. CONCLUSIONS

Electrostatic force between bacteria and NPs must take in consideration as samples with negative hall coefficient have a bactericidal effect on Gram (+) bacteria, in contrast to samples with positive hall coefficient. In consequence, it is possible to expect the antimicrobial properties from the gradient in electron energy or a gradient in electrical potential where this mechanism involves a basic excitation process as an interaction between electrons and the lattice vibrations of the crystal. The band theory must take in consideration as it may give a qualitative result in the analysis the antimicrobial properties. Initial bacteria adhesion is recognized to be the essential step for biofilm formation. As the material is negatively charged, this may reduce bacteria attachment anddelay biofilm formation. Material with positively charged surface attract bacteria and therefore this electrostatic force disrupt surface growth. Most implantation failure come from bacterial infection, positively charged surfaced may control this drawback. We think that this work offer a probability avenue to control the microbial growth as this study search for a relation between electronic properties of (Sn-Bi) alloy and its antimicrobial properties. Doping alloys with nanoparticles consider a good avenue to protect surface from bacterial contamination but in future cytotoxity of nano used must be highlighted.

5. REFERENCES

1. Rashid, F. L., Hadi, A., Al-Garah, N. H., & Hashim, A. (2018). Novel phase change materials, MgO nanoparticles, and water based nanofluids for thermal energy storage and biomedical applications. *Int Pharmaceu Phytopharmacol Res*, *8*, 46-56.
2. Elahi, N., Kamali, M., & Baghersad, M. H. (2018). Recent biomedical applications of gold nanoparticles: A review. *Talanta*, *184*, 537-556. https://doi.org/10.1016/j.talanta.2018.02.088.
3. Sharma, G., Kumar, A., Sharma, S., Naushad, M., Dwivedi, R. P., ALOthman, Z. A., & Mola, G. T. (2017). Novel development of nanoparticles to bimetallic nanoparticles and their composites: a review. *Journal of King Saud University-Science*. https://doi.org/10.1016/j.jksus.2017.06.012.
4. Lux, F., Tran, V. L., Thomas, E., Dufort, S., Rossetti, F., Martini, M., ... & Boschetti, F. (2019). AGuIX® from bench to bedside—Transfer of an ultrasmall theranostic gadolinium-based nanoparticle to clinical medicine. *The British journal of radiology*, *92*(1093), 20180365. https://doi.org/10.1259/bjr.20180365.
5. Sahoo, S. K., Misra, R., & Parveen, S. (2017). Nanoparticles: a boon to drug delivery, therapeutics, diagnostics and imaging. In *Nanomedicine in Cancer* (pp. 73-124). Pan Stanford.
6. Sedki, M., Hassan, R. Y., Hefnawy, A., & El-Sherbiny, I. M. (2017). Sensing of bacterial cell viability using nanostructured bioelectrochemical system: rGO-hyperbranched chitosan nanocomposite as a novel microbial sensor platform. *Sensors and Actuators B: Chemical*, *252*, 191-200. https://doi.org/10.1016/j.snb.2017.05.163.
7. Liu, J., Teng, J., Yun, K., Wang, Z., & Sun, X. (2019). Investigation of thermodynamic and shape memory properties of alumina nanoparticle-loaded graphene oxide (GO) reinforced nanocomposites. *Materials & Design*, 107926. https://doi.org/10.1016/j.matdes.2019.107926.
8. Li, J., Rao, J., & Pu, K. (2018). Recent progress on semiconducting polymer nanoparticles for molecular imaging and cancer phototherapy. *Biomaterials*, *155*, 217-235.Shaw, L., Luo, H., Villegas, J., & Miracle, D. (2004). *Processing and properties of mechanical alloyed Al93Fe3Cr2Ti2 alloys*. CONNECTICUT UNIV STORRS. https://doi.org/10.1016/j.biomaterials.2017.11.025.
9. Silhavy, T. J., Kahne, D., & Walker, S. (2010). The bacterial cell envelope. *Cold Spring Harbor perspectives in biology*, *2*(5), a000414. https://doi.org/10.1101/cshperspect.a000414.
10. Roberts, I. S. (1996). The biochemistry and genetics of capsular polysaccharide production in bacteria. *Annual Reviews in Microbiology*, *50*(1), 285-315. https://doi.org/10.1146/annurev.micro.50.1.285.
11. Hamouda, T., & Baker Jr, J. R. (2000). Antimicrobial mechanism of action of surfactant lipid preparations in enteric Gram-negative bacilli. *Journal of applied microbiology*, *89*(3), 397-403. https://doi.org/10.1046/j.1365-2672.2000.01127.x.
12. Fu, H., Yang, X., Jiang, X., & Yu, A. (2014). Silver vanadate nanobelts: a highly sensitive material towards organic amines. *Sensors and Actuators B: Chemical*, *203*, 705-711. https://doi.org/10.1016/j.snb.2014.07.057.
13. Teixeira, A. B. V., Vidal, C. L., Albiasetti, T., de Castro, D. T., & dos Reis, A. C. (2019). Influence of Adding Nanoparticles of Silver Vanadate on Antibacterial Effect and Physicochemical Properties of Endodontic Sealers. *Iranian Endodontic Journal*, *14*(1), 7-13. https://doi.org/10.22037/iej.v14i1.22519.
14. Wang, L., Hu, C., & Shao, L. (2017). The antimicrobial activity of nanoparticles: present situation and prospects for the future. *International journal of nanomedicine*, *12*, 1227. https://doi.org/10.2147/IJN.S121956.
15. Rezić, I., Haramina, T., & Rezić, T. (2017). Metal nanoparticles and carbon nanotubes—perfect antimicrobial nano-fillers in polymer-based food packaging materials. In *Food Packaging* (pp. 497-532). Academic Press. https://doi.org/10.1016/B978-0-12-804302-8.00015-7.
16. Roduner, E. (2006). Size matters: why nanomaterials are different. *Chemical Society Reviews*, *35*(7), 583-592. https://doi.org/10.1039/b502142c.
17. Abdelghany, A. M., Meikhail, M. S., Abdelraheem, G. E. A., Badr, S. I., & Elsheshtawy, N. (2018). Lepidium sativum natural seed plant extract in the structural and physical characteristics of polyvinyl alcohol. *International Journal of Environmental Studies*, *75*(6), 965-977. https://doi.org/10.1080/00207233.2018.1479564.
18. Singh, D. P., Polychronopoulou, K., Rebholz, C., & Aouadi, S. M. (2010). Room temperature synthesis and high temperature

frictional study of silver vanadate nanorods. *Nanotechnology*, *21*(32), 325601. https://doi.org/10.1021/ja047846d.
19. Dutta, A. K., Jarero, G., Zhang, L., & Stroeve, P. (2000). In-situ nucleation and growth of γ-FeOOH nanocrystallites in polymeric supramolecular assemblies. *Chemistry of Materials*, *12*(1), 176-181. https://doi.org/10.1021/cm990522h.
20. McAlister, S. P., & Hurd, C. M. (1979). Hall effect in 3d-transition metals and alloys. *Journal of Applied Physics*, *50*(B11), 7526-7530. https://doi.org/10.1063/1.326888.
21. Ando, T., Fowler, A. B., & Stern, F. (1982). Electronic properties of two-dimensional systems. *Reviews of Modern Physics*, *54*(2), 437. https://doi.org/10.1103/RevModPhys.54.437.